ATMOSPHERIC PRESSURE PLASMA JET IN ARGON GAS DRIVEN BY USING NEON SIGN TRANSFORMERS

Truong Thi Hoa
University of Technology and Education - The University of Danang

ARTICLE INFO

Received: 04/02/2025
Revised: 08/4/2025
Published: 12/4/2025

KEYWORDS

Atmospheric pressure plasma jet
Non-thermal plasma
Neon sign transformer
Dielectric barrier discharge
High voltage discharge

ABSTRACT

In this study, atmospheric pressure plasma jet was generated by a high-frequency, high-voltage source modulated by a neon sign transformer. Neon transformers are compact, cost-effective, and have ability to generate high-frequency output voltage, which makes them particularly effective for generating argon-based plasma jets. The main focus is on evaluating the effects of continuous voltage modulation by the neon sign transformer on the electrical characteristics of atmospheric pressure plasma jets in Ar gas. It is found that alterations in the modulated voltage also alternate plasma intensity. Changes in voltage amplitude in each modulation cycle of the neon sign transformer leads to significant changes in the electrical characteristics of the plasma jets. Furthermore, an increase in voltage amplitude not only enhances plasma intensity but also corresponds to a nearly linear increase in power consumption and dissipation within the treated targets. By examining these parameters, the study seeks to provide insights into optimizing plasma generation for energy-efficient and high-performance applications in fields such as biomedical treatments, agriculture, and food safety.

ĐẶC TÍNH TIA PLASMA ÁP SUẤT KHÍ QUYỂN TRONG KHÍ ARGON ĐƯỢC TẠO RA BẰNG CÁCH SỬ DỤNG MÁY BIẾN ÁP NEON

Trương Thị Hoa
Trường Đại học Sư phạm Kỹ thuật - Đại học Đà Nẵng

THÔNG TIN BÀI BÁO

Ngày nhận bài: 04/02/2025
Ngày hoàn thiện: 08/4/2025
Ngày đăng: 12/4/2025

TỪ KHÓA

Plasma áp suất khí quyển
Plasma lạnh
Máy biến áp neon
Phóng điện màn chắn điện môi
Phóng điện cao áp

TÓM TẮT

Trong nghiên cứu này, tia plasma áp suất khí quyển đã được tạo ra bởi bởi máy biến áp Neon. Máy biến áp Neon có kích thước nhỏ gọn, chi phí thấp và có thể tạo ra điện áp cao, tần số cao nhằm vận hành hiệu quả hệ thống tia plasma trong môi trường khí Argon. Mục tiêu chính của nghiên cứu là tạo ra tia plasma bởi nguồn điện có chi phí hợp lý dễ vận hành, đồng thời đánh giá ảnh hưởng của việc thay đổi biên độ điện áp liên tục bởi máy biến áp Neon đối với các đặc tính điện của tia plasma trong khí Ar. Kết quả thí nghiệm cho thấy sự thay đổi trong biên độ điện áp ở mỗi chu kỳ điều biến của nguồn điện dẫn đến những thay đổi đáng kể trong đặc tính điện học của các tia plasma. Hơn nữa, sự tăng biên độ điện áp không chỉ làm tăng cường độ plasma mà còn tương ứng làm tăng gần như tuyến tính các giá trị điện năng tiêu thụ của hệ thống và sự tiêu hao năng lượng trên mục tiêu được xử lý. Các kết quả nghiên cứu cung cấp thông tin chi tiết về khả năng tối ưu hóa quá trình tạo ra tia plasma với hiệu suất cao ứng dụng trong các lĩnh vực như điều trị y sinh, nông nghiệp và an toàn thực phẩm.

DOI: https://doi.org/10.34238/tnu-jst.11959

Email: tthoa@ute.udn.vn

1. Introduction

Atmospheric pressure plasma jet (APPJ) is non-thermal plasma that operates at atmospheric pressure conditions, where electron temperature is much higher than heavy particle temperature. They contain a variety of reactive species, such as reactive oxygen and nitrogen species (RONS). These devices are widely valued for their application in sensitive areas such as biomedical treatments, agriculture, and food safety without causing thermal damage [1], [2]. APPJs are extensively employed in biomedical applications, including sterilization, wound healing, and cancer therapy, owing to their ability to deliver RONS that exhibit antimicrobial and cytotoxic effects [2]. Moreover, APPJs have shown exceptional potential to promote seed germination and early seedling development by modulating biochemical and physiological responses in plants [3], [4]. In food safety, APPJs have been utilized to inactivate pathogens while preserving the nutritional quality of food [5].

APPJs configuration typically utilize coaxial dielectric barrier discharge (DBD) configurations, where dielectric layers are placed between electrodes to prevent arcing and ensure stable plasma formation. In most studies, Argon, a noble gas, which offers lower breakdown voltage and enhanced discharge stability, widely used as a working gas for plasma generation [6] – [8]. APPJs based on DBD systems exhibit distinct electrical behaviors depending on the working gas, electrode configuration, and power source. Emerging studies have emphasized the influence of electrical parameters, such as pulse duration, frequency, and voltage amplitude, on plasma characteristics. The properties of the dielectric material and the different power supply methods will affect the stability and energy efficiency of DBD-driven plasma jet [9] – [13].

Neon sign transformers are devices widely used in lighting systems for neon signs and are high-voltage devices designed to drive gas discharges. They operate by converting industrial sinusoidal alternating current main voltage into high voltage with high frequency, sufficient to ionize working gases. Neon transformers are compact, cost-effective, and have high-frequency output voltage, which makes them particularly effective for generating argon-based APPJs [14]. A standard output voltage waveform of a neon sign transformer (NST) characterized by its high-frequency, high-voltage sinusoidal oscillations. The waveform appears to have a modulated envelope that the voltage amplitude increases to a peak before decreasing, which repeats cyclically and is composed of multi-sinusoidal waveforms [13].

This study aims to explore the characteristics of Ar-APPJs driven by a NST. The modulation in amplitude of output voltage waveforms plays a pivotal role in controlling the properties of the plasma. Therefore, the research on the impact of voltage amplitude modulation on plasma characteristics within the output voltage envelope of a neon transformer reveals the progression of plasma development under various amplitude modulations. The investigation focuses on key relationships between applied voltage, discharge current, total power consumption, and power dissipation on target surfaces. By examining these parameters, the research seeks to provide insights into optimizing plasma generation for energy-efficient and high-performance applications.

2. Experimental setup

The experimental setup for APPJ is illustrated in Figure 1, showing (a) the schematic diagram of the setup, (b) the structure of electrodes and reactor, and (c) the wiring diagram. The experimental condition is shown in Table 1. The reactor is a quartz tube with dimensions of 6.5 mm inner diameter, 8.8 mm outer diameter, 110 mm length, and 2 mm wall thickness. A high voltage electrode is a copper wire positioned in the center of the discharge tube. The grounded electrode is a spiral wire located at the outer surface of the tube. A primary power supply generates a standard AC-50 Hz voltage (V_{in}) fed to the NST, which converts it into high voltage (V_{out}) with a rated value of 9 kV and a frequency of 17 kHz. The high voltage from the transformer is measured using a high-voltage probe (Tektronix P6015A 75 Mhz). The circuit

current is measured via a shunt resistor (BPC10100J 10Ω 10 W). The plasma jet is formed at the nozzle with Ar gas supplied from the upper of the tube as the working gas. Argon gas is introduced into the discharge tube by adjusting the flow rate at 1slm. At the exit of the reactor, a copper plate measuring 40 x 40 mm is positioned to direct the plasma, the plasma jet is emitted from the jet source and directed onto a copper plate. The copper plate in the setup serves as the target for the plasma jet. The accumulated charge on the copper plate is measured using a monitor capacitor (C_m) with capacitance of 1.3 nF. The voltage and current through the capacitor can be monitored using a high voltage probe (Tektronix P6015A 75 Mhz) and a current probe (CT- pearson 2877- 200 Mhz) connecting to the oscilloscopes. This setup facilitates the acquisition of Lissajous Figures, enabling the analysis of electrical parameters, such as plasma voltage and charge transfer characteristics. The voltage and current waveforms are observed and recorded by digital oscilloscopes (Tektronix MDO3022- 200 MHz-2.5G S/s and Tektronix TBS 1102B-EDU-100 MHz- 2.5G S/s).

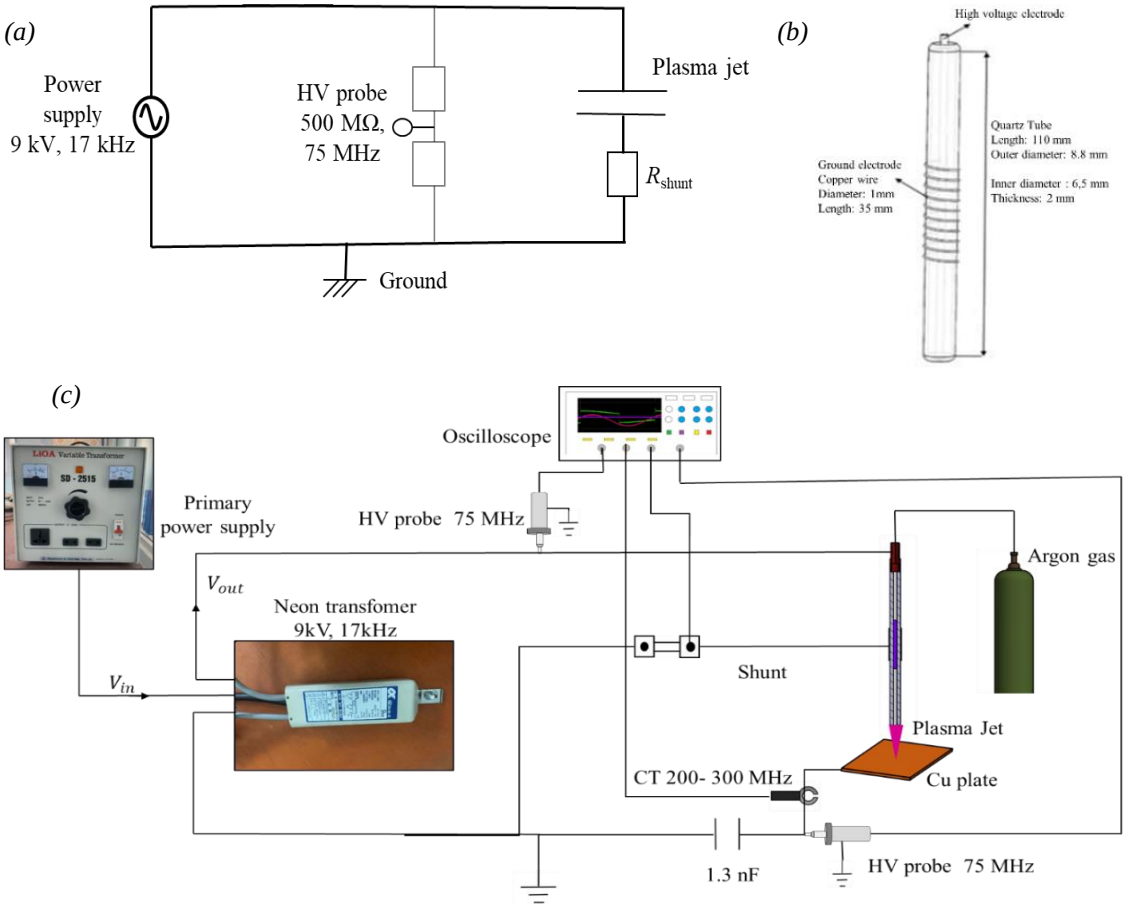

Figure 1. *Experimental setup: (a) schematic diagram, (b) reactor structure, (c) wiring diagram*

Table 1. *Experimental conditions with high frequency Neon sign transformer*

Primary power supply	0÷ 230 V, 50Hz
Neon transformer	0÷9 kV, 17 kHz
Working gas	Argon
Gas flow rate	1 slm
Pressure	Atmospheric pressure
Sample rate	2.5 GSa/s

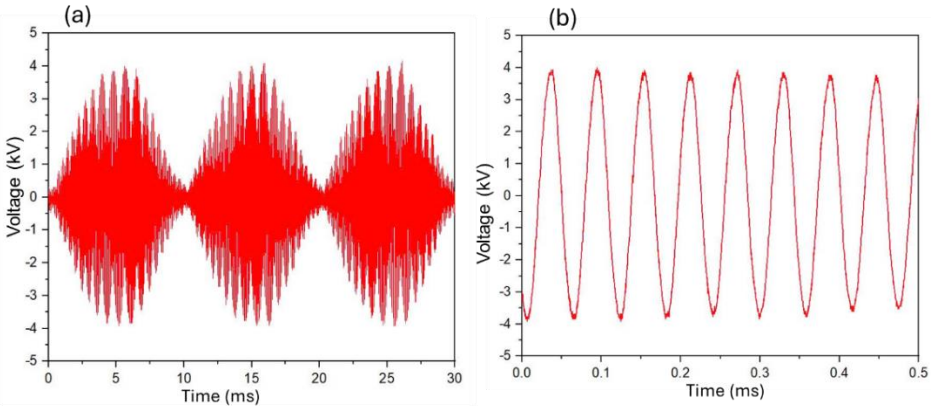

Figure 2. *The output waveforms of NST with* $V_{p\text{-}p}$ = 8 kV, 17.46 kHz: *(a) Waveform overview, (b) Enlargement waveform*

3. Experimental results and discussion

In the experimental NST exhibited maximum voltage amplitudes of 9 kV at frequencies of 17.46 kHz with a standard output voltage waveform shown in Figure 2. The waveform appears to have a modulated envelope showing that the voltage amplitude increases to a peak with $V_{p\text{-}p}$ = 8 kV before decreasing to $V_{p\text{-}p}$ = 0 kV, which repeats cyclically and being composed of multi-sinusoidal waveforms. Figure 3 presents the experimental results, which include the source voltage, discharge current, current through the measuring capacitor, and the voltage across the monitor capacitor. In this experimental condition, in each applied voltage envelope, the discharge just occurred when the voltage modulation applied to the high voltage electrode of the reactor started to reach an amplitude of $V_{p\text{-}p}$ = 4 kV or higher. Therefore, Figure 3 shows the discharge progress from 4 to 8 kV of the applied voltage peak. The discharge phenomenon occurs at the rising and falling edges corresponding to each half-cycle of the source voltage. Discharges mainly occur just before the voltage reaches its maximum value during the rising and falling edges of the supply voltage. Charges from the plasma jet accumulate on the oriented copper plate and are measured by the monitor capacitor (C_m = 1.3 nF). The current through the capacitor is related to the accumulated charges on the copper plate and voltage dropped on the capacitor is induced, exhibiting a waveform similar to that of the source voltage. As the applied voltage amplitude increases, the system observes a rise in both the number of discharge pulses and the peak value of the discharge currents. There is a clear enhancement in the intensity and frequency of current discharge spikes, with more pronounced and frequent spikes. A discharge current with a peak value of 54 mA was observed in the case of $V_{p\text{-}p}$ = 4 kV, then increased to a peak nearly 300 mA in the case of $V_{p\text{-}p}$ = 8 kV. At higher voltage levels, discharge currents are generated more frequently, and the discharge duration is extended. As a result, the capacitor captures a larger current than at lower voltage levels due to the accumulation of charges from the increased plasma current peaks (I). The trend in electrical properties, including the highest current pulse and the number of discharges at each voltage level, is illustrated in Figure 4. It demonstrates a quasi-linear relationship with changes in voltage amplitude. This indicates that the plasma intensity varies in accordance with the changes in voltage amplitude during one modulation cycle of the source voltage.

The temporary power $p(t)$ can be calculated by Equation (1) while energy (E) provided for the system in each cycle can be calculated by Equation (2). In these equations, v(t) and i(t) are voltage and current curves obtained by data acquisition system shown in Figure 3. The p(t) curves are shown in Figure 5 and energies (E) consumed in each cycle are areas bounded by the p(t) curves.

$$p(t) = v(t)i(t) \quad (1)$$

$$E = \int_0^T p(t)dt \quad (2)$$

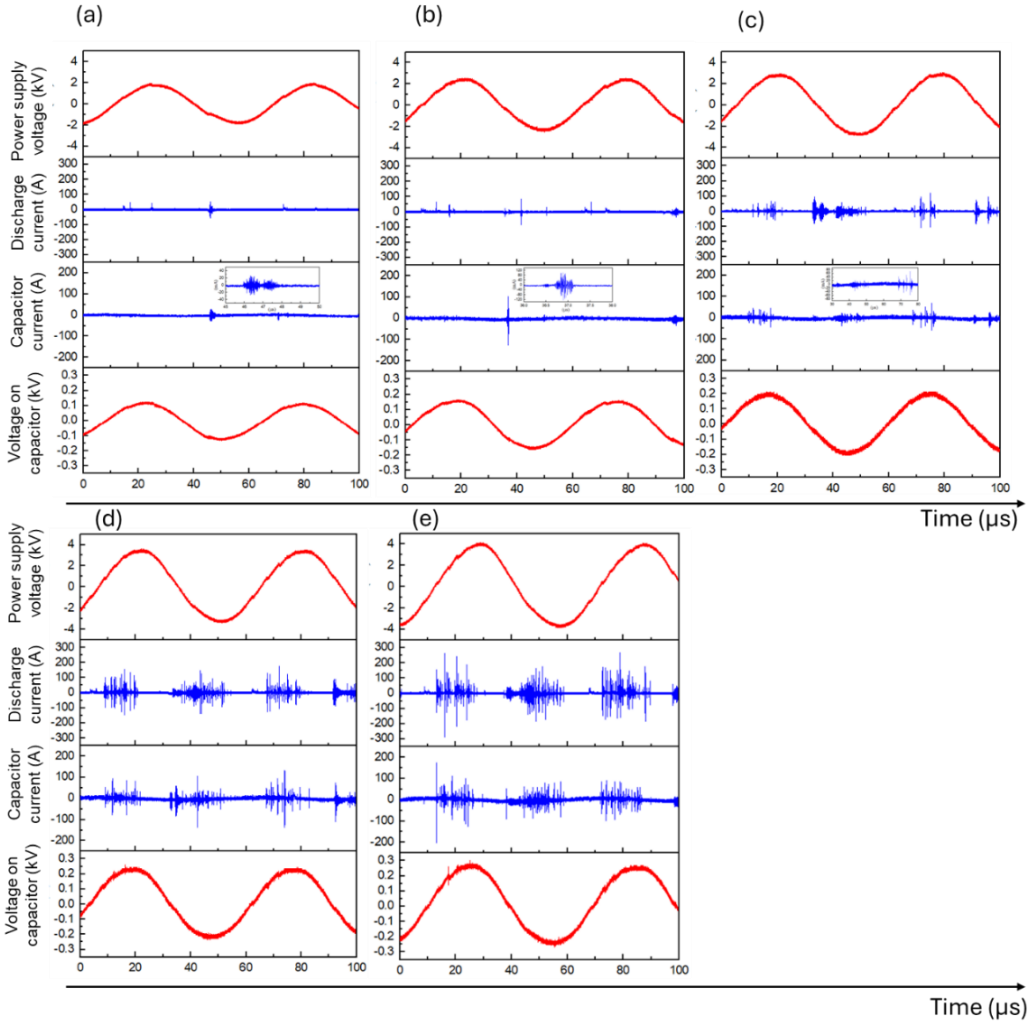

Figure 3. *Electrical characteristics of plasma jet within peak-to-peak voltage amplitude (V_{p-p}) modulation progress: (a) V_{p-p} = 4 kV, (b) V_{p-p} = 5 kV, (c) V_{p-p} = 6 kV, (d) V_{p-p} = 7 kV, (e) V_{p-p} = 8 kV*

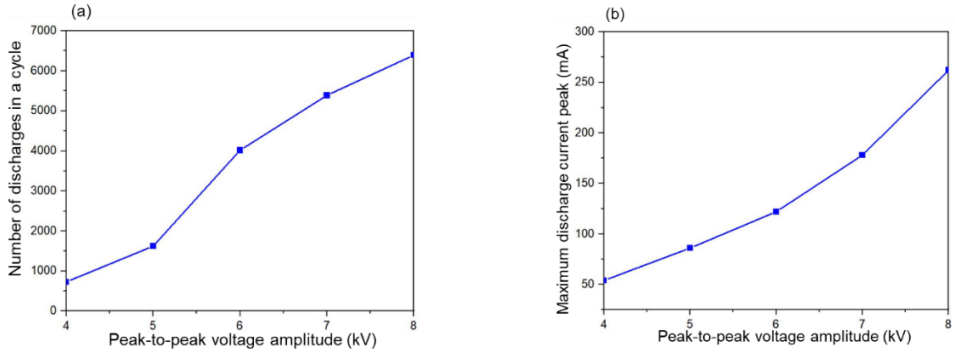

Figure 4. *Effect of peak-to-peak voltage amplitude on (a) discharge pulse density (counted when discharge current I ≥ 10 mA), and (b) maximum current discharge peak value*

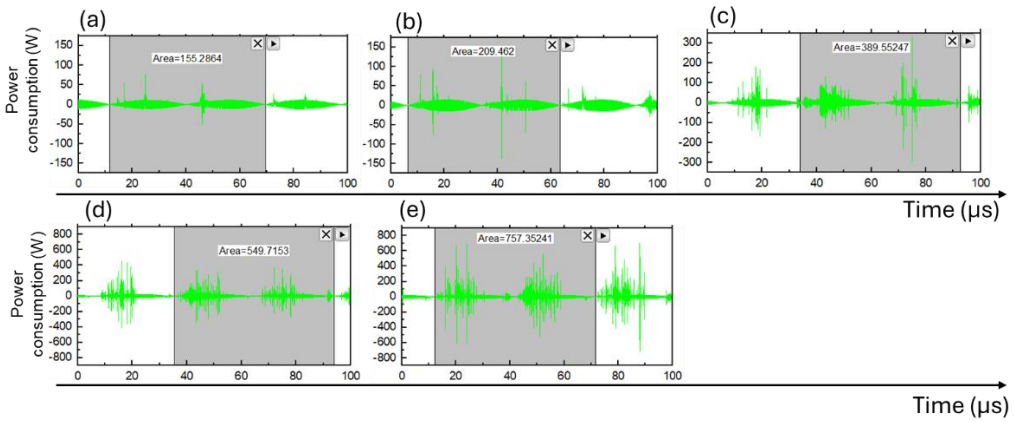

Figure 5. *Power and energy consumption during discharge cycles within peak-to-peak voltage amplitude ($V_{p\text{-}p}$) modulation progress: (a) $V_{p\text{-}p}$ = 4 kV, (b) $V_{p\text{-}p}$ = 5 kV, (c) $V_{p\text{-}p}$ = 6 kV, (d) $V_{p\text{-}p}$ = 7 kV, (e) $V_{p\text{-}p}$ = 8 kV*

The Lissajous diagram is a valuable tool to calculate the active power dissipated during discharge cycles, the method involves determining the area enclosed by the hysteresis loop in the charge-voltage (*Q-V*) diagram [14]. This relationship can be obtained by placing a capacitor (C_m) in series in the discharge circuit and plotting the voltage drop (v_m) across or charges variation (Q_m) on the capacitor against the voltage applied to the high voltage electrode (v_a). In a dielectric barrier discharge (DBD) system, the charge on the dielectric changes in response to variations in the applied voltage throughout the AC cycle, creating a loop. The area (*S*) encompassed by the *Q-V* hysteresis loop is directly related to the energy dissipated during each cycle of the AC voltage as Equations. (3-5). The average active power dissipated during plasma discharge can be calculated using Equation (6). Lissajous diagram and energies (E_d) dissipated on treatment target of copper plate in each cycle are shown in Figure 6.

$$Q_m(t) = C_m v_m(t) \tag{3}$$

$$i(t) = C_m \frac{dv_m(t)}{dt} \tag{4}$$

$$P(t) = v_a(t).i(t) = v_a(t) \cdot C_m \frac{dv_m(t)}{dt} \tag{5}$$

$$\overline{P} = \frac{1}{T}\int_0^T v_a(t) \cdot C_m \frac{dv_m(t)}{dt} dt = \frac{1}{T}\int_0^T v_a \cdot C_m dv_m = \frac{1}{T}\oint_{one\ cycle} v_a dQ_m = fS \quad (6) \text{ or } E_d = S \tag{6}$$

where *T* and *f* are period and frequency of power supply, respectively.

The power and energy provided by the NST during each cycle increase as the voltage amplitude increases, demonstrating the plasma enhancement effect that results from increasing voltage amplitude in a modulated envelope of the power supply voltage (Figure 7a). The plasma enhancement is also evidenced by the increased energy dissipation on the target treatment of the oriented copper plate (Figure 7b), reflecting how the elevated voltage amplitude in the power supply's modulated envelope intensifies the effects on the oriented copper plate. Increasing the voltage amplitude supplied to the APPJ could enhance the efficiency of processes such as material treatment or chemical synthesis, where more active plasma facilitates better interaction with materials. However, the enhancement also suggests higher instability, which could pose challenges in controlling the plasma characteristics for precise treatment.

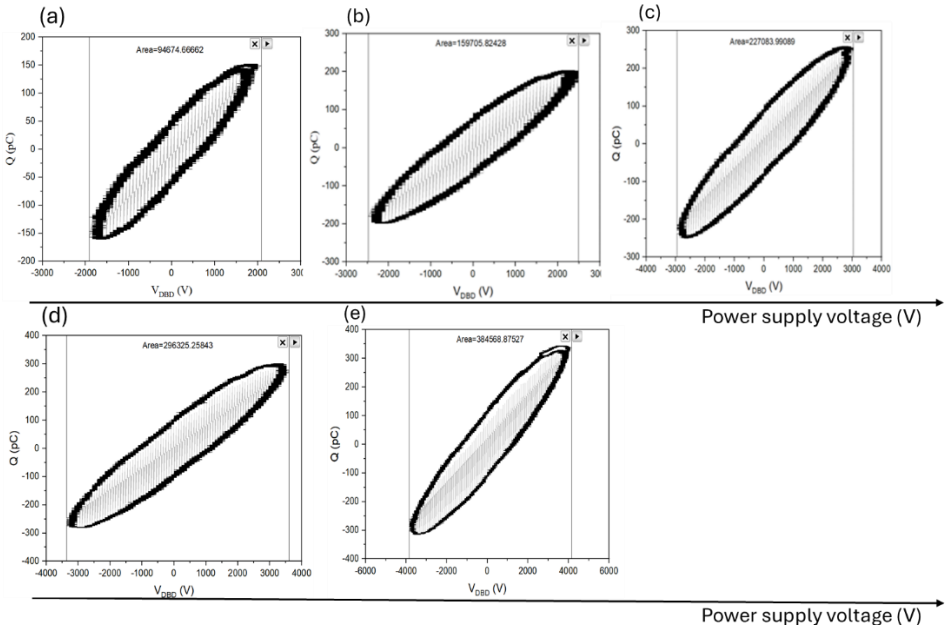

Figure 6. *Lisajous diagram and energy dissipation during discharge cycles on the target within peak-to-peak voltage amplitude (V_{p-p}) modulation progress (a) V_{p-p} = 4 kV, (b) V_{p-p} = 5 kV, (c) V_{p-p} = 6 kV, (d) V_{p-p} = 7 kV, (e) V_{p-p} = 8 kV*

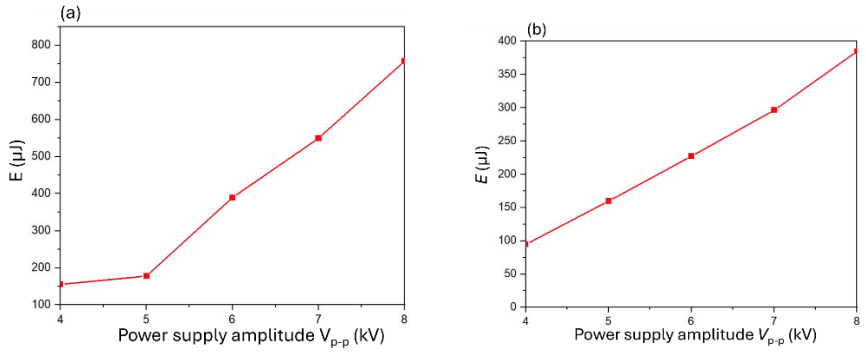

Figure 7. *Effect of peak-to-peak voltage amplitude (V_{p-p}) on (a) energy provided by power supply, and (b) energy dissipation on the treatment target*

4. Conclusion

In conclusion, this study has successfully demonstrated the generation of APPJ using a high-frequency, high-voltage source modulated by an NST. Systematic examination reveal that continuous voltage modulation from the NST significantly influences the electrical characteristics of APPJ in Ar gas. Specifically, variations in the modulated voltage directly affects the plasma intensity and stability, resulting in notable changes in the electrical behavior of the jet throughout each voltage cycle used to ignite the jet. Furthermore, an increase in voltage amplitude not only enhances plasma intensity but also leads to a nearly linear increase in power consumption and power dissipation on the treatment targets. It is important to note that within the voltage envelope of the NST, plasma only occurs when the peak-to-peak voltage (V_{p-p}) exceeds 4 kV, and its intensity increases until it reaches the maximum value of V_{p-p}. Consequently, there are periods when plasma does not occur and periods where plasma activity is very intense. This characteristic should be considered for specific applications, especially those requiring precise control over plasma properties such as in material treatment or chemical synthesis. In addition, these findings underscore the important role of voltage modulation in optimizing plasma jet performance for

various application scenarios, highlighting the need for careful control and understanding of the electrical parameters that affect plasma behavior. In addition, future research using variable frequency setups canoffer deeper insights into how frequency impacts the optimization of plasma processes. Optical emission spectroscopy should be investigated, incorporating practical experiments to evaluate the effectiveness of plasma applications, such as sterilization or surface treatment, thereby improving applications in plasma technology.

REFERENCES

[1] J. Winter, R. Brandenburg, and K-D. Weltmann, "Atmospheric pressure plasma jets: an overview of devices and new directions," *Plasma Sources Sci. Technol*., vol. 24, 2015, Art. no. 064001.

[2] M. Laroussi *et al.,* "Low-Temperature Plasma for Biology, Hygiene, and Medicine: Perspective and Roadmap," *IEEE Trans. Radiat. Plasma Med. Sci*., vol. 6, no. 2, pp. 127-157, 2022.

[3] O. B. Dhakal, R. Dahal, T. R. Acharya, P. Lamichhane, S. Gautam, B. Lama, R. khanal, N. K. Kaushik, E. H. Choi, and R. Chalise, "Effects of spark dielectric barrier discharge plasma on water sterilization and seed germination," *Current Applied Physics*, vol. 54, pp. 49-58, 2023.

[4] D. Cui, Y. Yin, J. Wang, Z. Wang, H. Ding, R. Ma, and Z. Jiao, "Research on the Physio-Biochemical Mechanism of Non-Thermal Plasma-Regulated Seed Germination and Early Seedling Development in Arabidopsis," *Front. Plant Sci*., vol. 10, 2019, Art. no. 1322.

[5] Y. Pan, J.-H. Cheng, and D.-W. Sun, "Cold Plasma-Mediated Treatments for Shelf Life Extension of Fresh Produce: A Review of Recent Research Developments," *Comprehensive Reviews in Food Science and Food Safety*, vol. 18, no. 5, pp. 1312-1326, 2019.

[6] R. Brandenburg, “Corrigendum: Dielectric barrier discharges: progress on plasma sources and on the understanding of regimes and single filaments,” *Plasma Sources Sci. Technol*., vol. 26, 2017, Art. no. 053001.

[7] E. J. Baek, H. M. Joh, S. J. Kim, and T. H. Chung, "Effects of the electrical parameters and gas flow rate on the generation of reactive species in liquids exposed to atmospheric pressure plasma jets," *Physics of Plasmas.*, vol. 23, 2016, Art. no. 073515.

[8] V. Horvatic, A. Michels, N. Ahlmann, G. Jestel, D. Veza, C. Vadla, and J. Franzke, "Time- and spatially resolved emission spectroscopy of the dielectric barrier discharge for soft ionization sustained by a quasi-sinusoidal high voltage," *Anal Bioanal Chem.*, vol. 407, no. 22, pp. 6689-6696, 2015.

[9] J.-S. Oh, H. Furuta, A. Hatta, and J. W. Bradley, "Investigating the effect of additional gases in an atmospheric-pressure He plasma jet using ambient mass spectrometry," *Jpn. J. Appl. Phys*., vol. 54, 2015, Art. no. 01AA03.

[10] A. Ivankov, T. Capela, V. Rueda, E. Bru, H. Piquet, D. Schitz, D. Florez, and R. Diez, "Experimental Study of a Nonthermal DBD-Driven Plasma Jet System Using Different Supply Methods," *Plasma.*, vol. 5, no. 1, pp. 75-97, 2022.

[11] F. Peeters and T. Butterworth, "Electrical Diagnostics of Dielectric Barrier Discharges," *Atmospheric Pressure Plasma – From Diagnostics to Applications*, 2019, pp. 1–33.

[12] G. He, Y. Liu, F. He, J. Miao, and J. Li, "Interaction between atmospheric pressure plasma jet and target," *Physics of Plasmas*, vol. 31, 2024, Art. no. 083503.

[13] M. F. Crowe, "Neon Signs: Their Origin, Use, and Maintenance," *The Journal of Preservation Technology*, vol. 23, no. 2, pp. 30-37, 1991.

[14] D. E. Ashpis, M. C. Laun, and E. L. Griebeler, "Progress Toward Accurate Measurements of Power Consumptions of DBD Plasma Actuators," *50th AIAA Aerospace Sciences Meeting including the New Horizons Forum and Aerospace Exposition*, Nashville, Tennessee, AIAA Report No.20120823, 2012.